

# **Radio Astronomical Instrumentation And Analysis Techniques**

Written Documentation submitted to the University of Delhi  
for PHYS-579



BY  
**Vinay Pravin Bharambe**

under the supervision of **Prof. T. R. Seshadri and Prof. H.P. Singh**

Department of Physics And Astrophysics

University of Delhi

Delhi-110 007

INDIA

(Submitted: May 2023)

Certain commercial entities, equipment, references or materials may be identified in this document in order to describe an experimental procedure or concept adequately. Such identification is not intended to imply recommendation or endorsement by the Department of Physics and Astrophysics, Delhi or Author, nor is it intended to imply that the entities, materials, or equipment are necessarily the best available for the purpose.

**MSc(Final), Department of Physics and Astrophysics,  
Delhi University, 43 pages,  
May 2023**

**This document is available free of charge from:**

**<https://github.com/VinayBharambe/MScF>**

**The programs executed in the following write up can be found at**

**<https://github.com/VinayBharambe/MScF>**



**Recommended:** The document contains animated graphics and it is recommended to use javascript enabled pdf viewer to have full experience, such as Adobe or KDE-Ocular.

# Abstract

Radio astronomy is a branch of Astrophysics which makes observations of astronomical sources at Radio wavelengths. It is a young branch of astronomy if compared with optical astronomy but still around 90 years old. First Radio observation of an astronomical source was done by Karl Jansky at Bell laboratories in 1932. Since, then this subject has flourished and is a workhorse in current Astronomy and Astrophysics research. Unlike other parts of electromagnetic spectrum the Earth's atmosphere is transparent to a big band of Radio frequencies. This makes ground based observations possible and more effective. Also, due to longer wavelengths Radio observations do not face problems due to intergalactic medium and cosmological observations are also possible at low radio frequencies.

## **Part 1: Design, simulations and fabrication of Pyramidal Horn antenna for 1.4 GHz observations**

Unlike Optical and Infrared astronomy the receiver for the Radio astronomy is an Antenna. An Antenna is an electric device which can both transmit and receive electromagnetic signals. The structure of an Antenna can vary a lot depending on frequency range. One of the most prominently observed frequency range in low frequency Radio astronomy is 1.4 GHz. It is one of the longest wavelength observed in Astronomy. We aimed to Design a Radio telescope for frequency centered at 1.4GHz with 20dB antenna gain. We designed the waveguide, flaring and probe of the antenna. We optimized the size of the flaring (and hence overall antenna) with iteration program. We simulated the design over HFSS simulations to study its radiation pattern and simulated gain. We fabricated 4 of such antennas. We designed and fabricated probe for these antennas. We designed the electronic receiver chain for the antenna and tested the software backend to modify observation conditions such as gain, frequency range, bandwidth, etc and to store the observations in a file. In the end we propose a concept to design a two element interferometer.

## **Part 2: Search for FRBs in uGMRT and SRT observations**

Fast Radio Bursts are Radio astronomical transients that are highly energetic in nature and lasts for millisecond duration. Since, it's first discovery in 2007 (Lorimer et al., 2007) many efforts have been made to detect, localize and follow up FRBs. While most of the FRBs are observed as one of events some of them have been found to be repeating in nature. With latest results from CHIME the number has raised to 50 (Andersen, B. C. et al., 2023). FRB 20180916 is one of such interesting repeater which has observed periodicity of  $16.35 \pm 0.15$  days (Pilia M. 2021).

In this document we present general procedure of analyze of Radio astronomical data with the example of FRB dataset. We also present work on the FRB search pipelines and effort to improvise SPANDAK pipeline. We present drawbacks and shortcomings of earlier pipelines and how SPANDAK helps improve the detection of FRBs.

# Contents

|  |           |
|--|-----------|
| <b>1 Basic structure of a Radio Telescope</b>                    | <b>1</b>  |
| 1.1 Introduction   | 1         |
| 1.2 1.4 GHz Radio Band   | 3         |
| 1.3 Pyramidal Horn Antenna                                       | 3         |
| 1.3.1 Waveguide  | 4         |
| 1.3.2 Flarings   | 7         |
| 1.3.3 Probe Parameters   | 10        |
| 1.4 Fabrication and actual dimensions                            | 11        |
| <b>2 Simulations of Pyramidal Horn on HFSS</b>                   | <b>12</b> |
| 2.1 Network Parameter simulations                                | 12        |
| 2.1.1 S - Parameter  | 12        |
| 2.1.2 Y - Parameter  | 13        |
| 2.1.3 Z - Parameter  | 13        |
| 2.1.4 VSWR   | 14        |
| 2.2 Far field simulations  | 15        |
| 2.2.1 Gain (Total)   | 15        |
| 2.2.2 Directivity  | 16        |
| 2.2.3 Realized Gain  | 17        |
| 2.2.4 Other Plots  | 18        |
| <b>3 Electronic system for the telescope</b>                     | <b>19</b> |
| 3.1 General structure of Electronic system for a Radio telescope | 19        |
| 3.2 Electronics to be used with Horn antenna                     | 20        |
| 3.3 Software backend of the telescope                            | 21        |
| <b>4 Two element interferometer</b>                              | <b>23</b> |
| <b>5 Radio Astronomical Data</b>                                 | <b>26</b> |
| 5.1 Introduction   | 26        |

|          |   |           |
|----------|---|-----------|
| 5.2      | General steps of analysis of Radio astronomical data:     | 26        |
| 5.2.1    | Conversion of RAW data into usable format                 | 26        |
| 5.2.2    | Headers in the Observation                                | 27        |
| 5.2.3    | Identification of Radio Frequency Interference (RFI)      | 28        |
| 5.2.4    | Radio Frequency Interference (RFI) Removal                | 28        |
| 5.3      | Commonly used Techniques in Radio astronomy Data analysis | 30        |
| 5.3.1    | Fourier analysis  | 30        |
| 5.3.2    | Curve fitting and Gaussian analysis                       | 30        |
| 5.3.3    | Folding   | 30        |
| 5.3.4    | Match filtering   | 30        |
| <b>6</b> | <b>Fast Radio Bursts</b>                                  | <b>31</b> |
| 6.1      | Propagation effects                                       | 32        |
| 6.1.1    | Dispersion  | 32        |
| 6.1.2    | Scintillation   | 32        |
| 6.1.3    | Scattering  | 32        |
| 6.2      | FRB models  | 33        |
| 6.2.1    | Neutron star progenitors                                  | 33        |
| 6.2.2    | Black hole and White dwarf progenitor models              | 34        |
| <b>7</b> | <b>Search for FRBs in uGMRT and SRT Observations</b>      | <b>35</b> |
| 7.1      | RFI analysis  | 35        |
| 7.2      | Setting search Parameters                                 | 36        |
| 7.3      | Dedispersion  | 37        |
| 7.4      | Detection of the Candidates                               | 37        |
| 7.5      | Machine learning techniques                               | 37        |
| 7.6      | Plotting of the candidates                                | 38        |
| <b>8</b> | <b>FRB Software Jungle</b>                                | <b>39</b> |
| <b>9</b> | <b>By Products of FRB Analysis</b>                        | <b>41</b> |

|     |  |    |
|-----|--|----|
| 9.1 | Manual for installing SPANDAK on a latest Linux system | 41 |
| 9.2 | Common installer for Pulsar and and FRB repositories   | 41 |
| 9.3 | SPANDAK3   | 41 |

## List of Figures

|         |   |    |
|---------|---|----|
| Fig. 1  | A Single dish Radio telescope system (Source : Encyclopedia Britannica) | 1  |
| Fig. 2  | GMRT (Legacy) feeds   | 2  |
| Fig. 3  | Rectangular Waveguide   | 4  |
| Fig. 4  | TE10 mode   | 5  |
| Fig. 5  | Antenna theory by C. Balanis fig no. 13.16                              | 9  |
| Fig. 6  | Side View   | 11 |
| Fig. 7  | Four Horn Antennas  | 11 |
| Fig. 8  | S parameter   | 12 |
| Fig. 9  | Y parameter   | 13 |
| Fig. 10 | Z parameter   | 13 |
| Fig. 11 | Z parameter   | 14 |
| Fig. 12 | 3D Gain plot  | 15 |
| Fig. 13 | 2D Gain plot  | 15 |
| Fig. 14 | Spherical polar Directivity   | 16 |
| Fig. 15 | Directivity   | 16 |
| Fig. 16 | Realized Gain Plot  | 17 |
| Fig. 17 | Realized Gain Plot 2D   | 17 |
| Fig. 18 | Horn with radiation pattern   | 18 |
| Fig. 19 | Electronic system for Radio telescope (NCRA Blue book chapter 3)        | 19 |
| Fig. 20 | Electronic system for Radio telescope (Mhaske A. et al., August 2022)   | 20 |
| Fig. 21 | FM range Radio spectrum   | 22 |
| Fig. 22 | Two element interferometer (Chapter 4, NCRA Blue book)                  | 24 |
| Fig. 23 | ugmrt2fil   | 27 |

|                                   |    |
|-----------------------------------|----|
| Fig. 24 alex_uGMRT_make_header    | 27 |
| Fig. 25 pazi (PSRCHIVE)           | 29 |
| Fig. 26 FRB180916 observed by SRT | 38 |

## Part I

# **Design, Simulations and Fabrication of Pyramidal Horn antenna for 1.4 GHz**

# 1. Basic structure of a Radio Telescope

## 1.1 Introduction

A Radio telescope is an instrument which collects the radio signals from astronomical sources. Radio telescope can be a single dish or array of multiple antenna elements. Every Radio telescope consists of several components.

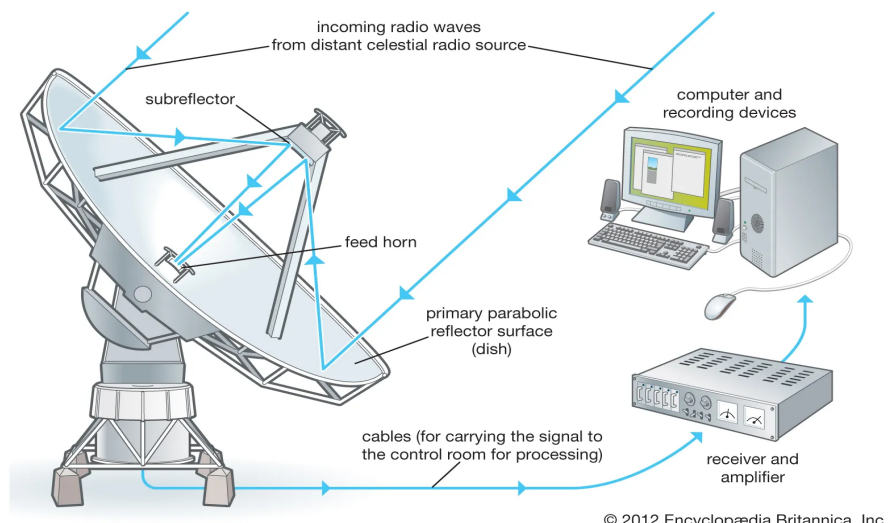


**Fig. 1.** A Single dish Radio telescope system (Source : Encyclopedia Britannica)

1. Dish or Reflector : It is a structure which collects the radio waves from the sky. The Dish is pointed in the direction of the source. The collected radio waves are then reflected back to the feed which points in direction of the reflector, The pointing of dish needs to be precise in order to receive maximum waves and reflect them to the feed.

2. Feed : A feed is the electric instrument which converts the electromagnetic waves into electric signals. The feeds can be of various shapes. It can be a monopole, dipole, microstrip antenna or as in case of 1.4 GHz, a Horn antenna. Below picture shows feeds from GMRT, Pune (Ananthakrishnan S., 2005). The feed in the 1 GHz to 1.4 GHz is a Corrugated Horn antenna.



**Fig. 2.** GMRT (Legacy) feeds

3. Receiver front end : The biggest challenge in observing astronomical signals is they are extremely weak. Before the electric signal is transmitted to back end it needs to be amplified. This needs to be done just after the antenna stage since even a small resistance can introduce enough noise to bury the signal in noise. This is done with Low Noise Amplifiers. Also, after the amplification sometimes a filters are also used to reject known high RFI (Radio frequency interference) channels. Using cooling systems for Front end electronics can remarkably reduce thermal noise in the system.
4. Mount : Like most optical telescopes, due to enormous size of the telescope it is only feasible to have an Alt-Az mount system. The size of fully steerable single dish radio telescope ranges from 10 m (South Pole Telescope) to the biggest 100 m (Green Bank Telescope). Servo motor systems are used for smooth movement of the telescope.

5. Transmission lines : The amplified signal is then transferred to the receiver back end with coaxial cables or optical fiber network. The distance between the two can be few kilometers.
6. Receiver back end : The Receiver back end forms the signal processing units and software back end.
7. Computing facility and storage systems : It includes real time tracking of the observations and monitoring of Antennas. The real time monitoring is very important for transient events such as FRBs.

## 1.2 1.4 GHz Radio Band

The 1.4 GHz frequency range is very interesting band in Radio astronomy. It is one of the longest wavelengths probed in Radio astronomy. The most important source of emission in 1.4 GHz range is 21 cm Neutral Hydrogen line. There exists many active and energetic sources at 21 cm which are possible to be observed by A small scale Horn Antenna. For example, 3C 461 (SNR-Cassiopeia A), 3C 405 (D Galaxy-Cygnus A), 3C 144 (SNR-Crab Nebula), 3C 145 (Emission Nebula-OrionA) etc. With interferometry techniques and using multiple antennas Pulsar observations from strong sources can also be tried.

## 1.3 Pyramidal Horn Antenna

An **Antenna** is an electric device which can both receive and transmit electromagnetic radiation. The size, shape and structure of an Antenna can vary a lot depending on its desired gain, frequency range and desired source of observation. The simplest antenna is a monopole antenna which is basically a copper wire which receives electromagnetic waves and downconverts them into electric signals. Few examples of the Antenna type are Long dipole, Helical antenna, Micro strip antenna, Reflector antenna, etc. A Pyramidal Horn antenna has 3 main components - Waveguide, Flaring and Probe.

### 1.3.1 Waveguide

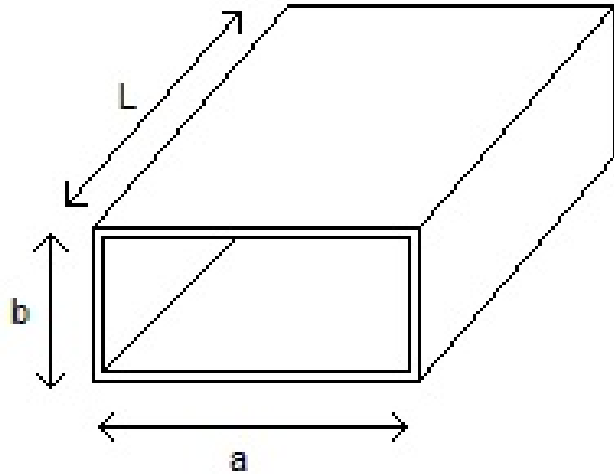


**Fig. 3.** Rectangular Waveguide

Waveguide is the part of the horn antenna where EM waves are transported from the antenna to the probe or feed. It does not have any gain but is just a high pass filter with very low losses to transport the wave to the electronics. Being a high pass filter it has a cutoff frequency.

We are going to operate our apparatus at 1420405751 Hz or 1420 MHz and we are going to receive red or blue shifted frequencies and **the high pass filter have factor of 1.25 times above cutoff frequency where the transfer function is maximum and the transfer is constant**. Also, there is a fraction after which the gain is not

So, we for our application choose  $f_c = 850$  MHz

$$\therefore f_{\text{low}} = f_c * 1.25 = 1062.5 \text{ MHz}$$

$$\therefore f_{\text{high}} = f_c * 1.89 = 1606.5 \text{ MHz}$$

Hence, the Horn antenna will function best in the range of about 1.1 GHz to 1.6 GHz. A closest commercial match to this Waveguide is **WR650**. It can be checked on [Pasterneck](#).

The Waveguide have various modes of operation. We will be operating the Waveguide in TE<sub>10</sub> mode. TE<sub>10</sub> mode has the lowest attenuation of all modes in a rectangular waveguide and its Electric field is vertically polarized.

Below figure shows that in TE<sub>10</sub> mode, the variation in E field is in one plane hence there is no variation in H field in perpendicular plane. Hence, a E-field varies sinusoidally along a and uniform along b. The variation along a is  $\frac{\lambda}{2}$ .

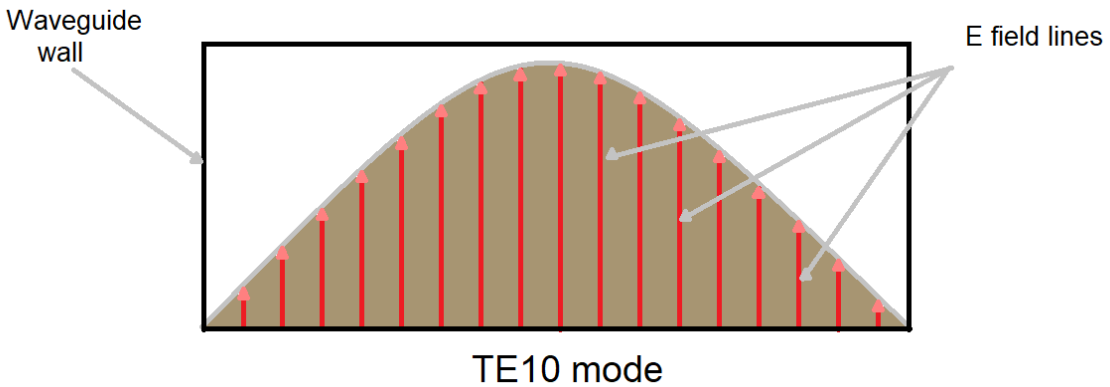


**Fig. 4.** TE10 mode

The cutoff frequency of a waveguide is given as

$$f_c = \frac{1}{2\sqrt{\mu\epsilon}} \sqrt{\left(\frac{m}{a}\right)^2 + \left(\frac{n}{b}\right)^2}$$

Since, We are operating in TE<sub>10</sub> mode,  $m = 1$ ,  $n = 0$  and let's use 'c'.

$$\therefore f_c = \frac{c}{2} \sqrt{\left(\frac{1}{a}\right)^2 + \left(\frac{0}{b}\right)^2}$$

$$\therefore 850 M = \frac{c}{2a}$$

$$\therefore a = \frac{c}{2 \times 850M}$$

$$\therefore a = 17.64 \text{ cm} \approx 6.94'' \approx 7''$$

Since, we have no dependence on  $b$ . ' $b$ ' can conveniently be chosen as half of  $a$ .

$$\therefore b = 8.82 \text{ cm} \approx 3.46'' \approx 3''$$

$\Rightarrow$  The design that we have decided to build is also almost the same and is perfect just the  $f_c$  will be 847 MHz

So,  $a = 17.7 \text{ cm}$  and  $b = 8.3 \text{ cm}$ . Now, Onwards I will be using these values and  $f_c = 847.4 \text{ MHz}$  or near to it.

The length of the Waveguide can be designed according to the wavelength of operating frequency. Here 1420405751 Hz

$$\lambda_g = \frac{\lambda}{\sqrt{1 - \left(\frac{f_c}{f}\right)^2}}$$

Where,

$$f_c = 847.45 \text{ MHz}$$

$$f = 1420405751 \text{ Hz}$$

$$\lambda = 21.10 \text{ cm}$$

$$\Rightarrow \lambda_g = 26.31 \text{ cm}$$

The Waveguide is air-filled waveguide hence, it has impedance of  $377\Omega$   
Further studies of impedance of waveguide with probe distance can be carried out later.

### 1.3.2 Flarings

To start with,

We have,

$$a = 17.7 \text{ cm}$$

$$b = 8.3 \text{ cm}$$

While the Gain of the antenna can be chosen according to the available electronics, one of the first work in this design was done by Patel N. A., Patel R. N. et al., at Harvard-Smithsonian Center for Astrophysics. They had tested the setup for 20dB gain and with available commercial RF components. Hence, We also decided the desired gain of the horn to be 20dB in order to have good directivity and under control sidelobe shapes.

Let us start with Gain ,

$$G_0(\text{dB}) = 20 = 10 \cdot \log_{10}(G_0)$$

$$\Rightarrow G_0 = 20 = 10^2 = 100$$

Now, we have ,

$$\left( \sqrt{2\chi} - \frac{b}{\chi} \right)^2 (2\chi - 1) = \left( \frac{G_0}{2\pi} \sqrt{\frac{3}{2\pi}} \frac{1}{\sqrt{2\pi}} - \frac{a}{\lambda} \right)^2 \left( \frac{G_0}{6\pi^3} \frac{1}{\chi} - 1 \right)$$

Let, the initial guess be

$$\chi_0 = \frac{G_0}{2\pi\sqrt{2\pi}} = \frac{100}{2\pi\sqrt{2\pi}} = 6.34936$$

$$a = 17.7 \text{ cm} = \frac{17.7}{21.20} = 0.8386\lambda$$

$$b = 8.3 \text{ cm} = \frac{8.3}{21.10} = 0.3932\lambda \text{ and } G_0 = 100$$

On running iterations from MATLAB program from Balanis book.

**For  $\chi_i = 6.0298$**

$$\Rightarrow \rho_e = \chi_i \lambda = 127.39 \text{ cm}$$

$$\Rightarrow \rho_h = \frac{G_0^2}{8\pi^3} \left( \frac{1}{\chi_i} \right) \lambda = 141.25 \text{ cm}$$

$$\Rightarrow a_1 = \sqrt{3\lambda\rho_2} \approx \sqrt{3\lambda\rho_h} = \frac{G_0}{2\pi} \sqrt{\frac{3}{2\pi\chi_i}} \lambda = 94.62 \text{ cm}$$

$$\Rightarrow b_1 = \sqrt{2\lambda\rho_1} \approx \sqrt{2\lambda\rho_e} = \sqrt{2\chi_i\lambda} = 73.37 \text{ cm}$$

$$\Rightarrow P_e = (b_1 - b) \left[ \left( \frac{\rho_e}{b_1} \right)^2 - \frac{1}{4} \right]^{\frac{1}{2}} = 108.19 \text{ cm}$$

$$\Rightarrow P_h = (a_1 - a) \left[ \left( \frac{\rho_h}{a_1} \right)^2 - \frac{1}{4} \right]^{\frac{1}{2}} = 108.19 \text{ cm}$$

$$\Rightarrow \psi_E = 16.735 \text{ Deg}$$

$$\Rightarrow \psi_H = 19.568 \text{ Deg}$$

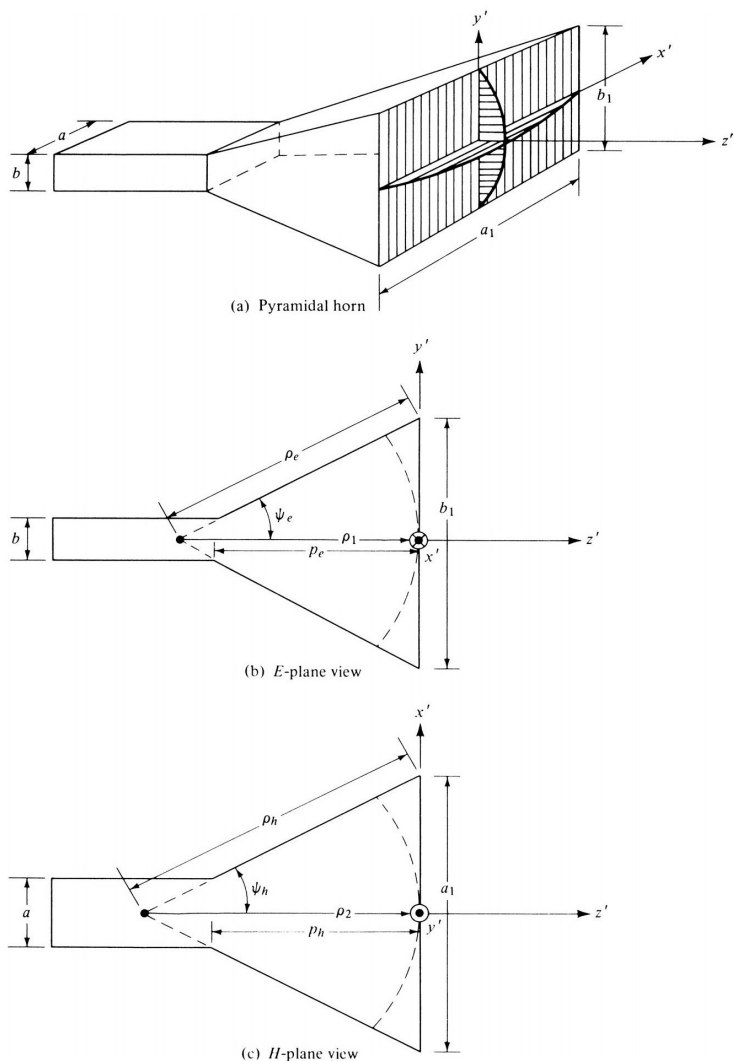


**Fig. 5.** Antenna theory by C. Balanis fig no. 13.16

$a_1$  and  $b_1$  : Waveguide dimensions,

$a_1$  and  $b_1$  : Flaring aperture dimensions,

$P_e$  and  $P_h$  : the base height

$\rho_e$  and  $\rho_h$  : slant height

$\psi_E$  and  $\psi_H$  : E and H plane flare angles

### 1.3.3 Probe Parameters

#### (1) Probe length

The probe is nothing but a monopole antenna.

For  $\lambda = 21.10$  cm, We should use  $\frac{\lambda}{4}$  length probe.

$$l = \frac{\lambda}{4} = \frac{21.10}{4} \approx 5.3 \text{ cm}$$

#### (2) Probe Distance

Probe distance is dependent on  $\lambda_g$

We have calculated  $\lambda_g$  in 1.3.1 and should ideally be

$$d = \frac{\lambda_g}{4} = \frac{26.3}{4} = 6.6 \text{ cm}$$

#### (3) Probe Radius

The efficiency of the horn will be dependent on the radius of monopole probe.

With increase in radius,bandwidth of monopole increases .

The ideal radius, as of now I can simulate with HFSS.

Also, different combinations of probe distance, radius can be tried and observed.

## 1.4 Fabrication and actual dimensions

We had chosen a good margin in desired gain to compensate for the fabrication uncertainties and errors. In fabrication had to change  $a_1$  by 1.4 cm and the final aperture width turned out to be 93.2 cm. We lost about 0.1 dB gain in this manipulation. With the simulations on the latest design the Total Gain = 20.19 dB.

All the other dimensions were very precise and error was within range of mm's for length dimensions and 1° for Flaring angles,



**Fig. 6.** Side View



**Fig. 7.** Four Horn Antennas

## 2. Simulations of Pyramidal Horn on HFSS

We performed simulations of the Pyramidal Horn antenna to study its Gain characteristics, Radiation pattern, Impedance-Admittance parameters etc. Here, we present the Simulation results of the Fabricated design. I have divided the study in two parts

### 2.1 Network Parameter simulations

We studied Scattering parameter, Admittance parameter and Impedance parameter of the Horn antenna. We also studied VSWR and Passivity of the antenna.

#### 2.1.1 S - Parameter

Scattering parameter forms elements of Scattering matrix which is one of the matrix solved to get antenna characteristics. It is closely related to VSWR of the Antenna. S parameter values help study linear characteristics of the Horn antenna. Below is the simulated S(1,1) - parameter characteristics for the 1.42 GHz Horn antenna. The graph shows S(1,1) Return loss of the system.

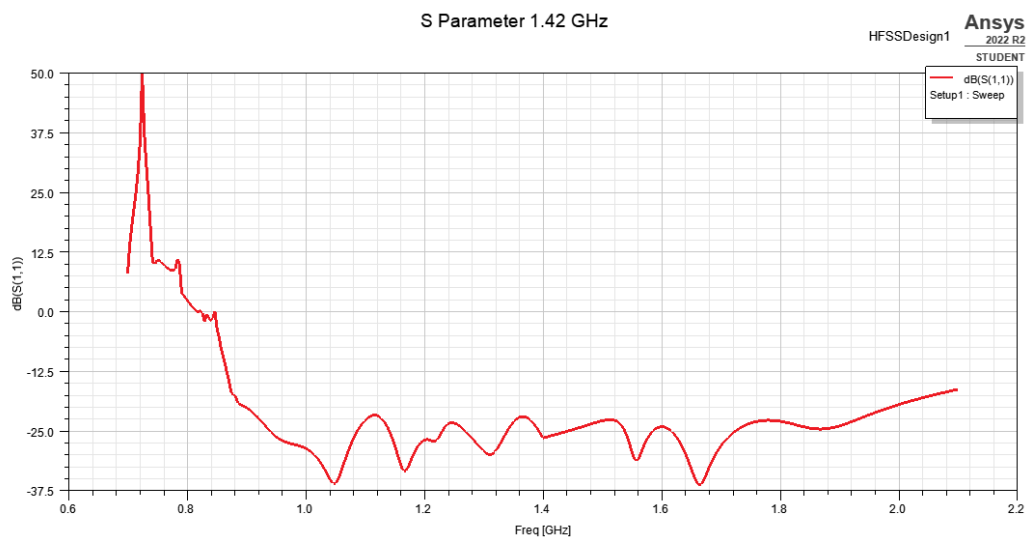


**Fig. 8.** S parameter

### 2.1.2 Y - Parameter

It is also known as Admittance parameter or elements which forms elements of Admittance matrix. Y parameters are also called as short circuit impedance because they are calculated in Short circuit conditions. It is difficult to measure Y and Z parameters reliably but still we can simulate there results in HFSS.



**Fig. 9.** Y parameter

### 2.1.3 Z - Parameter

They are similar to the Y parameters and describes behaviour of linear electric circuits. They are also known as Impedance parameters. It is difficult to measure Z parameters reliably but still we can simulate there results in HFSS.

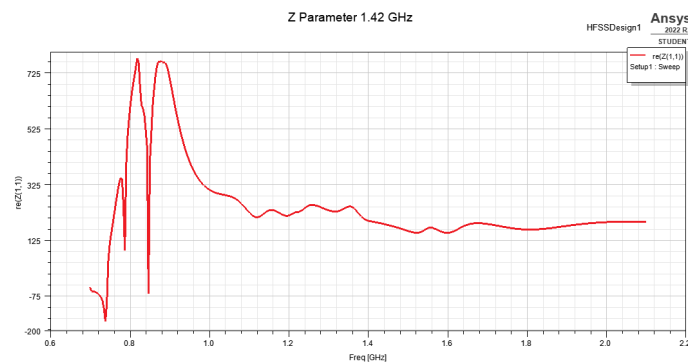


**Fig. 10.** Z parameter

## 2.1.4 VSWR

VSWR (Voltage Standing Wave Ratio) is a measure of how well the antenna impedance matches with the transmission line connected to it. It is given as

$$VSWR = \frac{1 + |\Gamma|}{1 - |\Gamma|}$$

Where  $\Gamma$  is another antenna parameter which is known as Reflection coefficient.

VSWR is the ratio of the peak amplitude of a standing wave to the minimum amplitude of a standing wave.

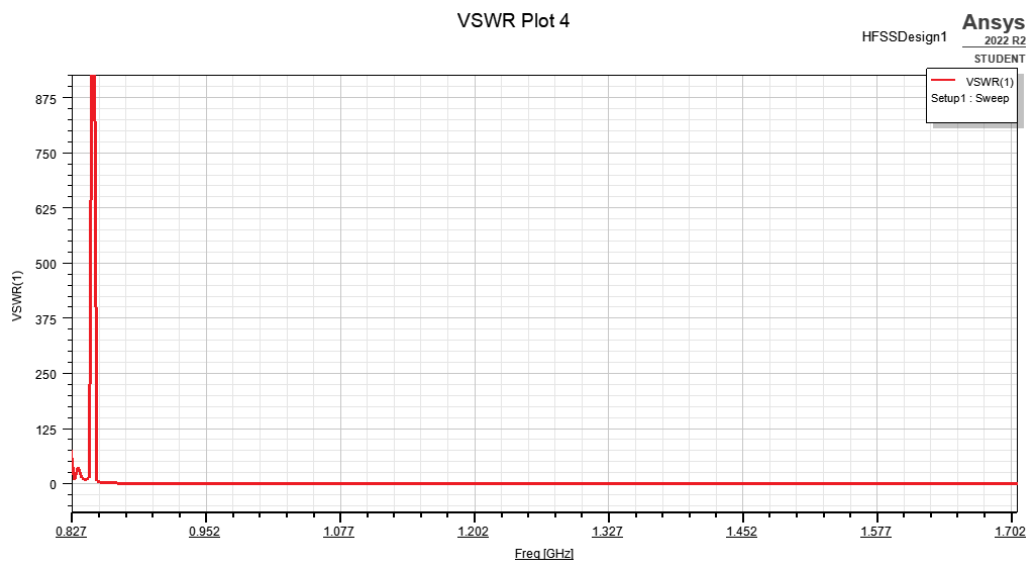


**Fig. 11.** Z parameter

## 2.2 Far field simulations

This includes 2D and 3D simulations of Gain, Realized Gain, Directivity of the antenna.

### 2.2.1 Gain (Total)

Gain represents the input power on the collecting area of the antenna. A better gain reflects to a good antenna. Amplifiers can be used to improve the signal quality but a bare minimum gain is required till the signal is fed to the electronic circuit. Fig 12 shows a 3D Polar plot of total Gain of the Antenna. The Azimuthal angle is Phi and Altitude angle is Theta.

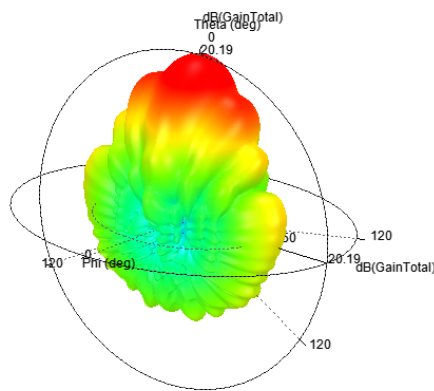


**Fig. 12.** 3D Gain plot

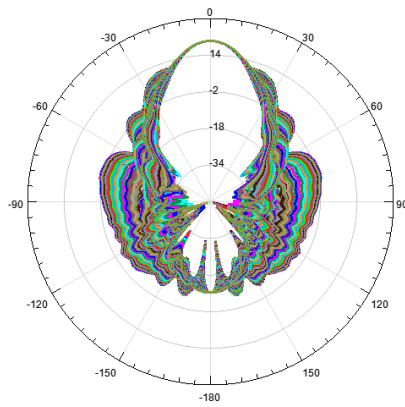


**Fig. 13.** 2D Gain plot

### 2.2.2 Directivity

Directivity is closely related to Gain of the antenna. Gain is the measure of the efficiency of the Antenna while Directivity only relates to the pattern and directional properties of antenna. Directivity analysis of the antenna is necessary for selection of the source and pointing of antenna. Below is the simulated behavior of the designed Horn antenna. The first is a spherical polar plot of the directivity of the antenna while second shows the variation in Theta and Phi direction.

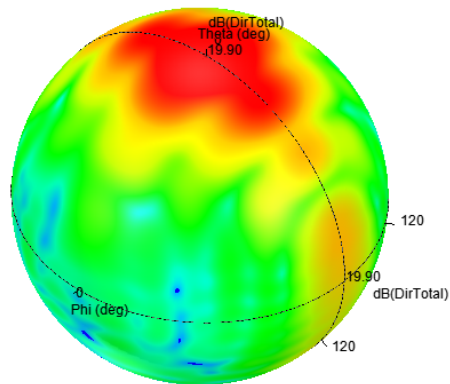


**Fig. 14.** Spherical polar Directivity

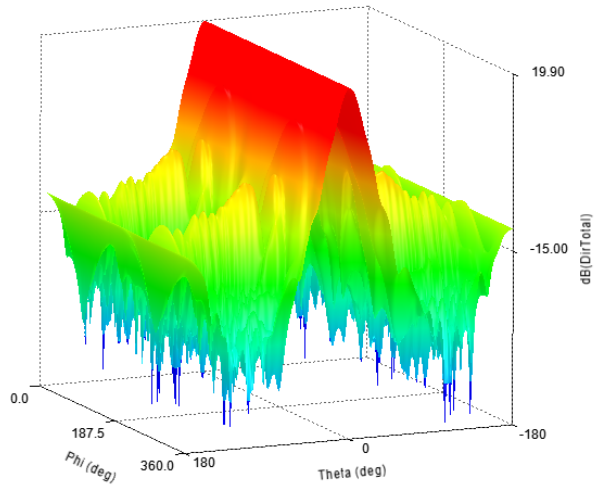


**Fig. 15.** Directivity

### 2.2.3 Realized Gain

The Realized Gain or absolute Gain is the Gain of an RF instrument which is reduced by a factor of impedance mismatch. Below fig 16 is a contour map of Realized Gain for the designed Horn antenna. Also Fig 17 is the two dimensional Realized Gain plot which shows the effective range of Theta to observe a radio source.

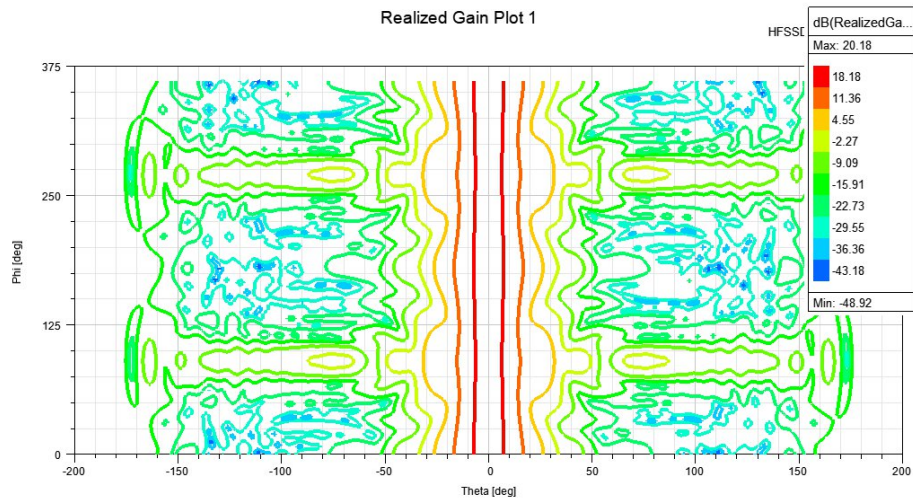


**Fig. 16.** Realized Gain Plot

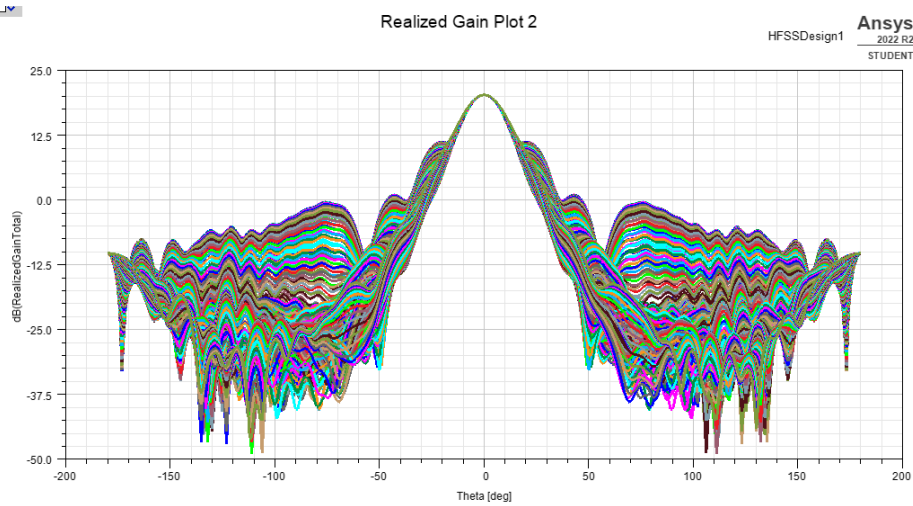


**Fig. 17.** Realized Gain Plot 2D

## 2.2.4 Other Plots

### 1. Horn Antenna with Radiation field

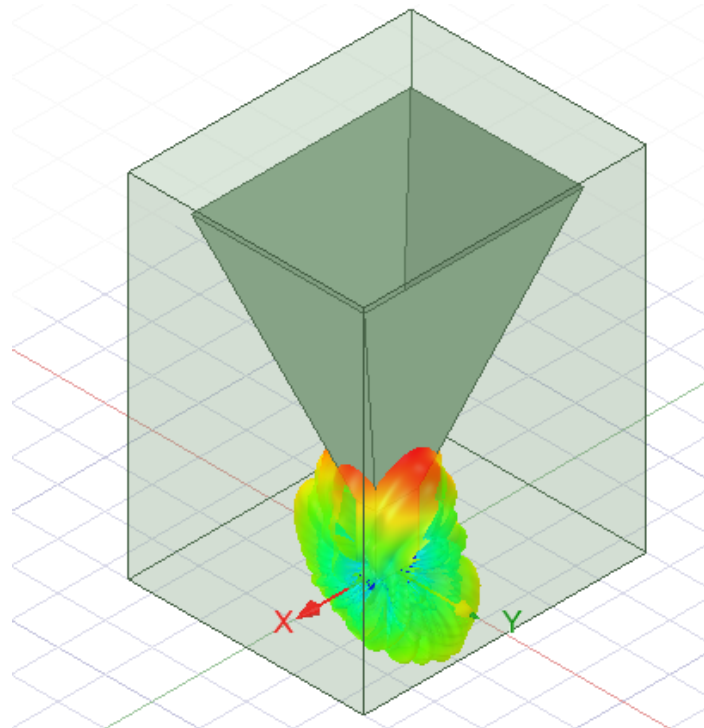


**Fig. 18.** Horn with radiation pattern

### 3. Electronic system for the telescope

The biggest challenge in receiving astronomical radio signals is they are very weak. Hence, a considerable amount of work is needed to be done on the received signal before it can be of any scientific importance.

#### 3.1 General structure of Electronic system for a Radio telescope

The Electromagnetic waves received from the sky are converted into electric signal by the feed of the antenna. Since the signal is very weak before doing any operation on the signal it needs to be amplified. This is done with Low Noise Amplifiers (LNAs). Low noise amplifiers are special type of amplifiers which only amplifies low power signal. Hence, noise from the signal remains as it is and only astronomical signal is amplified. It is necessary to have LNA stage exactly after the feed. Any other resistance introduced to signal will introduce thermal noise and it will be difficult to recover astronomical signal from it. LNAs are often provided with cooling systems to improve its thermal performance.

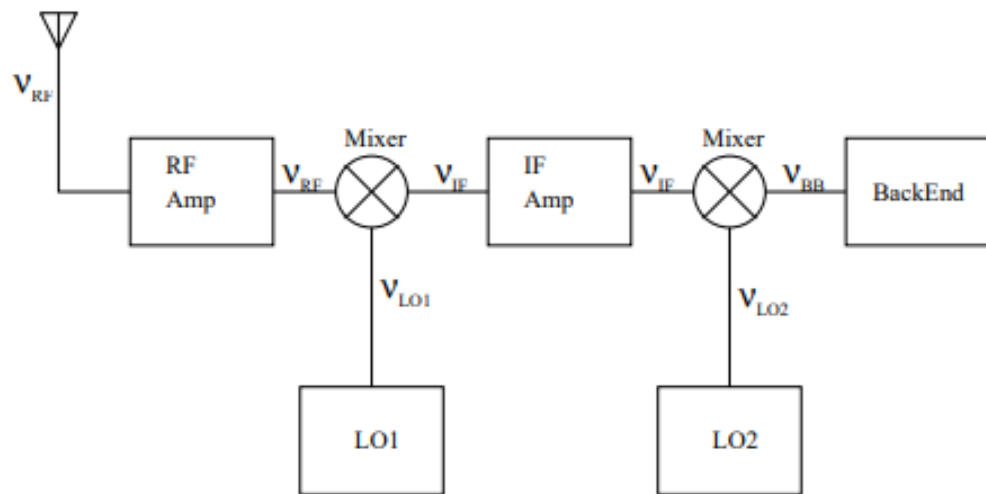


**Fig. 19.** Electronic system for Radio telescope (NCRA Blue book chapter 3)

The amplified signal is then fed to mixer stage where the signal is changed to an intermediate frequency by using a local oscillator. This is useful method as it helps you use same electronic backend for different observation frequencies. Sometimes more than one stages of mixer are used to minimise transmission losses. This is called as “Super-heterodyne system”. On Amateur scale some of these tasks can be performed by an SDR (Software Defined Radio).

Sometimes a band pass filter is used in Amateur Radio systems to only pass required observation frequency. Many times a certain range Band stop filter is used to block known RFI (Radio Frequency Interference).

### 3.2 Electronics to be used with Horn antenna

We will be using a very commonly used Electronic setup for receiver. Below image shows a block diagram of the same.

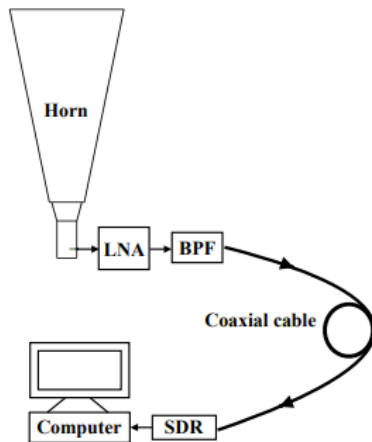


**Fig. 20.** Electronic system for Radio telescope (Mhaske A. et al., August 2022)

We will be using a common purpose LNA with a wide band Band pass filter centered around 1.42 GHz. Further with requirement to extend the coaxial cable few stages of RF amplifiers can be installed (which are currently unavailable to us). Lastly, an SDR can be used to monitor, record, plot and control input parameters such as Bandwidth, Integration time of the antenna.

### 3.3 Software backend of the telescope

Software Defined Radio has simplified and reduced cost of small scale Radio setup remarkably. This has led to form many SDR communities and forums through out the world. Apart from Third party software developed by SDR manufacturers there exists number of open source programs to tune, monitor, record, control SDR. They allows us to change Bandwidth and Integration time of the receiver.

The minimum detectable temperature by a Radio telescope is limited by the Antenna and the receiver electronics. It is given as

$$\Delta T_{min} = \frac{k_s T_{sys}}{\sqrt{\Delta v t n}}$$

Here,

$T_{sys}$  : System temperature

$\Delta v$  : Bandwidth

t : Time of integration

n : number of records averaged

System Temperature is the numerical quantity which measures the thermal equivalence of the system noise. The system includes the Antenna and the electronic systems. Increasing time of integration and Bandwidth helps improve the observation quality and hence decrease the  $\Delta T_{min}$

We will be using a RTL-SDR over anaconda base. We will be using software tool called “rtl\_power” by Kyle Keen to record and control the bandwidth, time of integration, length of observation, Subsequently we’ll be using heatmap.py to observe the waterfall plots of the observations. More post processing can be done with other open source programs. GNURadio and pyrtlsdr are the most used one.

Few more GUI based programs like rtl\_sdrpan or even commercial programs like CubicSDR can be used for live observations.

Below is a waterfall plot of the FM range recorded with the CubicSDR. It shows otherwise silent spectrum except a FM channel showing the signature at around 95MHz. One can also see USB (Upper side band) and LSB (Lower side band) of the FM signal. The antenna used was 5 cm monopole antenna.

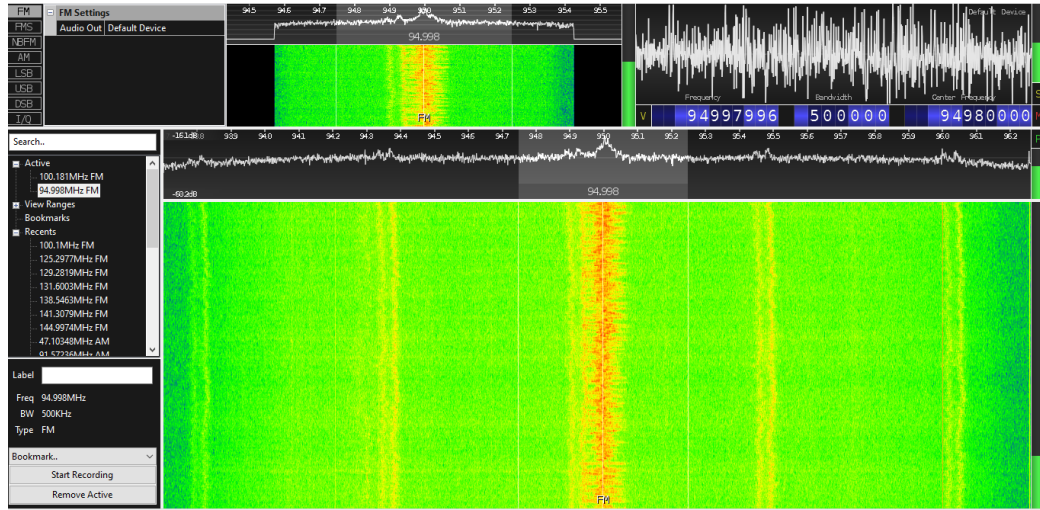


**Fig. 21.** FM range Radio spectrum

## 4. Two element interferometer

The observation of Neutral Hydrogen 21 cm line is an simple and elegant experiment. The Northern hemisphere has many prominent radio sources at 1.42 GHz frequency. Also, Observation of Hydrogen in Galactic plane is also one of the important target of observation. While most of these observations can be done with a single antenna, the observations are extremely limited by the collecting area and the resolution of the Antenna. This is where interferometry becomes important. The goal of designing these antennas is to achieve interferometry and extend the observations to other objects. Also, improve the observation quality of the Galactic plane observations.

The resolution of the observation is limited by the Aperture of the telescope. It is theoretically limited to

$$\theta \approx \frac{\lambda}{D}$$

To observe an object at certain frequency with higher resolution will require to increase the Diameter of the telescope. For Radio wavelengths this Diameter can go to few to hundreds of kilometers to achieve same resolution that a meter class optical telescope can give. To solve this problem, In 1952 Martin Ryle and Derek Vonberg came up with the first two element Radio interferometer. With interferometry same resolution can be achieved with multiple telescopes separated by a distance ‘D’.

We plan to extend our work towards first building a two element interferometer and observe sources in galactic plane with improved resolution. Further, with all our 4 Horn antennas we can greatly improve both resolution and collecting area of the telescope array to achieve greater results.

In a Radio interferometer, the ‘n’ number of telescopes are pointed towards the same source and observed simultaneously. But since it is not a single telescope and there is finite distance between two telescopes there is a phase difference. The delay occurs due to geometrical distance and needs to be negated before hand. This is done with electronic delay. Below figure shows a representation of local oscillators and integration of both signals in a two element interferometer.

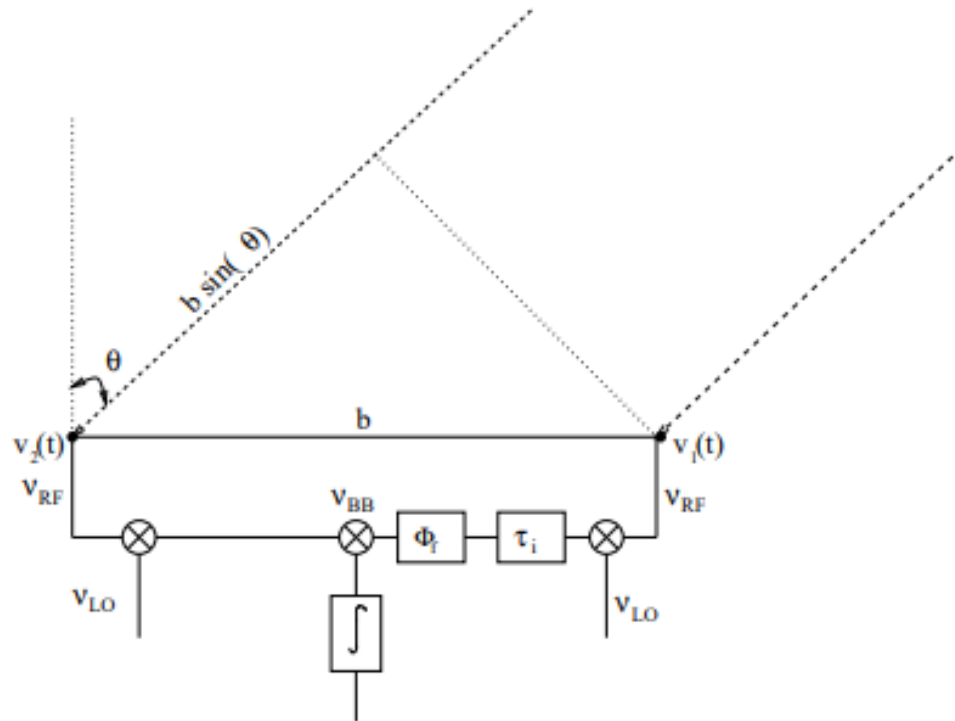


**Fig. 22.** Two element interferometer (Chapter 4, NCRA Blue book)

A four element interferometer will be more complex and the best orientation of the array can be calculated and simulated (with HFSS).

## Part II

# **Search for FRBs in uGMRT and SRT observations**

# 5. Radio Astronomical Data

## 5.1 Introduction

Radio astronomical observations are done in various modes while the general procedure of processing remains the same. Radio astronomical data is huge in volumes and is now counted as one of the big data problem. The famous Black hole image by Event Horizon Telescope required Terabytes of data to be processed. Hence, Parallel processing and machine learning algorithms are used to help reduce the data set.

A Radio telescope is basically an antenna which stores voltages as a function of time. But this is repeated for all the channels. The size of the observation also depends on bandwidth.

## 5.2 General steps of analysis of Radio astronomical data:

### 5.2.1 Conversion of RAW data into usable format

The Data format of most telescope observatory differs from other. This is different encoding used to store data. Also, different Radio observations have different needs and hence different file formats exists in different Radio observations. For example, Pulsar and FRB astronomers mostly use filterbank files while Radio imaging astronomers use ‘.ms’ files. ms stands for “Measurement sets”. Even inside a same domain there exists different formats. For example, In FRBs few observatories prefer using PSRFITS format while few other uses PSRDADA format. This has led to many file formats across radio astronomy and the first step in analysing the data is to convert the RAW data into a file format of your use.

For uGMRT data, .LTA is the observatory format. For H1 line observations this file is converted in ti measurement sets using CAPTURE pipeline (Ruta Kale et al., October 2020). For FRBs and Pulsar observations uGMRT file needs to be converted into filterbank file. There exists number of programs for this conversion.

One of them is ugmrt2fil python program by Alessandro Ridolfi. Below is the image of ugmrt2fil conversion by the ugmrt2fil program.

```
vinay@trg1:/data3/vinay/12thNov_data$ ugmrt2fil -ugmrtfile FRB180916_bml_pa_500_200_8_12nov2020.raw.gmrt_dat -bitshift 4 -o FRB180916_bml_pa_500_200_8_12nov2020.fil
#####
# ugmr2fil #####
# 1.0.2 (30Apr2019) #
#####

UGMRT file to convert: 'FRB180916_bml_pa_500_200_8_12nov2020.raw.gmrt_dat'

=====
Observation Properties:
=====
    Source name: FRB180916
        RA: 01:58:00.7502
        DEC: +65:43:00.3152
    Observing mode: Timing
        Array mode: CDP
        Num of channels: 2048
    Channel width (MHz): -0.09765625
Central freq. of first channel (MHz): 500.051171875
Lowest freq. of observing band (MHz): 300.1
Highest freq. of observing band (MHz): 500.1
Central freq. of observing band (MHz): 400.1
Total observing bandwidth (MHz): -200.0
    Sampling time (s): 8.192e-05
        Bits per sample: 16
    MJD of first time sample: 59164.83161372406
        Number of samples: 29712384
    Observation length: 2434.0984972800002

    Block size (bytes): 204800000
Original data size (bytes): 121701924864
Number of blocks to write = 594
Last bit of the observation to write (bytes) = 50724864
Writing output file 'FRB180916_bml_pa_500_200_8_12nov2020.fil' with 8 bits per sample with bitshift 4...
block #1 / 594 (0) ---> outfile size = 257 bytes (write speed = 0.00 MB/s | ETA: nan min)
block #2 / 594 (204800000) ---> outfile size = 102400257 bytes (write speed = 38.04 MB/s | ETA: 25.37 min)
```

**Fig. 23.** ugmrt2fil

### 5.2.2 Headers in the Observation

To convert a RAW file to measurement set or filterbank one needs to specify the observation details and few more details. This is done by providing the file with header information, For this reason one needs to generate a header file with the required details. For this task there also exists a number of programs. One of them is “alex\_uGMRT\_make\_header” by Alessandro Ridolfi. It inputs number of parameters such as source name, number of channels to be created, bandwidth of the channel, sampling time, Array mode etc. Time of observation is provided with .hdr file by the observatory. Below is an example of the command.

```
vinay@trg1:/data3/vinay/12thNov_data$ alex_uGMRT_make_header -hdr FRB180916_bml_pa_500_200_8_12nov2020.raw.hdr -o FRB180916_bml_pa_500_200_8_12nov2020.raw.gmrt_hdr -so
uncname=FRB180916_nchan=2048 Chanbw=-0.09765625 -fch1 300.1 -tsamp 81.92 -array_mode CDP -bitshift 4
--> IST: 2020-11-12 01:27:31.425758720
--> UTC: 2020-11-11 19:57:31.425758720
--> MJD: 59164.83161372406

Header file FRB180916_bml_pa_500_200_8_12nov2020.raw.gmrt_hdr successfully created!
```

**Fig. 24.** alex\_uGMRT\_make\_header

Number of channels (Nchan) Nchan represents number of channels to be created in the filterbank. It is usually in powers of 2. More the number of channels finer will be the resolution of the observation. While more number of channels are needs more processing time.

Sampling time It is the rate at which observations are made. Finer sampling time means more time resolution and hence more processing power. But every time fine sampling time is not useful. To Observe long time scale phenomenon sampling time needs to be more.

Channel bandwidth It is also one of the channel parameter, Number of channels x channel width is the total bandwidth of the observation.

**All the above parameter will be of use while observing with Horn antenna. A simple header program and conversion program can also be written for accommodating our Horn antenna observations into main stream Radio astronomy pipelines**

### **5.2.3 Identification of Radio Frequency Interference (RFI)**

Radio Frequency Interference is the biggest challenge to the Radio astronomical observations. This is because the RFI is often too strong as compared to astronomical signal and if it's frequency is coincident with astronomical signal, it will saturate the channel and astronomical signal will be lost. RFI also leads to false alarms and false signals in the observation. Telecom signals, nearby radar, Television or FM radio bands, electric transmission lines are main sources of the RFI. Hence, it is necessary to identify RFI. If it is consistent source then a Band stop filter can be used at the front end electronics of the Antenna. For other type of inconsistent RFI, various programs and algorithms are used.

### **5.2.4 Radio Frequency Interference (RFI) Removal**

There exists many RFI removal programs in every Radio astronomy field. For imaging Radio observation NRAO's "Common Astronomy Software Applications (CASA)" and "Astronomical Image Processing System (AIPS)" has common programs. For FRBs and

Pulsar observations “rfifind” program from PRESTO pipeline (Ransom et al. 2002) is an excellent program. It identifies RFI interference at Dispersion Measure 0 which are due to terrestrial phenomena. Further it removes the channels with RFI and improves the observation. The process of removing the channels is commonly called as “Zapping”.

Also, <https://psrchive.sourceforge.net/credits.shtml> has an excellent program “paz” which zaps the RFI channels. It’s improved version “pazi” (paz interactive) is an even better tool to visualize and manually zap the RFI channels. Below is an example of a pazi plot. It shows frequency against pulse phase channels. One can visually see horizontal lines which sweeps entire Pulse phase. These are RFIs and can be zapped interactively with *pazi*.

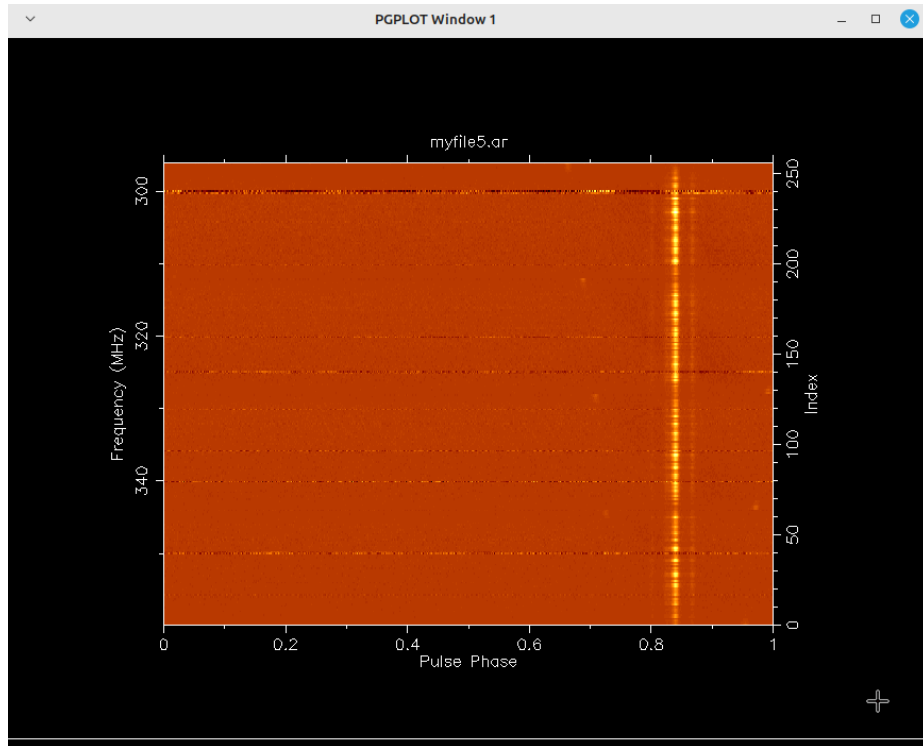


**Fig. 25.** pazi (PSRCHIVE)

Few more programs use other methods to identify the RFI. This includes removal of periodic RFI using Fourier transform techniques. Identifying RFI depending on its signature being repeated at different Dispersion Measures etc. Identification of RFI is an active research problem in Radio astronomy.

## **5.3 Commonly used Techniques in Radio astronomy Data analysis**

### **5.3.1 Fourier analysis**

Radio astronomical data analysis is very dependent on signal processing techniques. Fourier analysis is one of the most important method in image processing. It is used in enhancement analysis, restoration and compression. Discrete Fourier transforms are used to detect Pulsar features.

### **5.3.2 Curve fitting and Gaussian analysis**

Curve fitting is useful in studying statistical properties of the observation. The observations of the 21 cm Hydrogen line needs to be fitted with a Gaussian curve. This analysis gives information about Doppler shift of the source.

### **5.3.3 Folding**

Folding is a technique used in Pulsar astronomy which the observations are folded with a certain time interval. This is necessary because the intensity of the signal is very weak and pulsar signals are repeating in nature, Folding improved the Signal to noise ratio and hence makes detection easier.

### **5.3.4 Match filtering**

Match filtering is a technique in which for finding pulses in the data wider than a single time sample, the time series are convolved with boxcar functions of width W for multiple trial pulse durations. (Petroff E. et al. 2019)

## 6. Fast Radio Bursts

Pulsars have been a point of attraction for last 56 years. The Pulsar surveys of last few decades has given astronomers new marvels to wonder. Discovery of first millisecond pulsar was one of such discovery. After so many searches and observations there still remains few phenomenons such as Giant pulse, Pulse nulling, Profile mode changing which have not been settled yet. In 2007, radio pulsar survey by Lorimer et al. added to one more mystery in it. A very short duration, high intensity radio source was detected. From its characteristics it could not be linked to any existing Pulsar phenomenon. Subsequent more such candidates were reported by Keane et al. (2012), Petroff et al. (2015) and so on. In 2013 the term “Fast Radio Burst” was coined by Thornton et al. Since then more and more searches and observations are being made to detect, localize and follow up these sources. These are transient sources and have until now has no certain known origin.

Most of the current Radio telescopes are designed to look at a very small region of sky with high resolution. While FRBs are random in time and direction. Hence, for long time the FRB search was slowly moving ahead. Earlier few discoveries were with some of the surveys by Parkes Radio telescope. Transient nature also means there is need to observe the full sky and active monitoring, which requires enormous computing power. With Canadian Hydrogen Intensity Mapping Experiment (CHIME) telescope initiative opened to FRB observations the detection and follow up of FRBs has taken pace. CHIME has four 100 x 20 metre cylindrical parabolic reflectors and it observes in frequency range 400-800 MHz. The telescope cannot be moved and observes the sky as Earth rotates. CHIME has 1000 processor high performance GPGPU cluster which carries out computing operations.

Apart from CHIME other telescopes like LOFAR, Parkes, GBT, uGMRT, SRT etc also carries out FRB search observations in their capacity. Follow up observations, observations for repeating FRB or localization can be done with better accuracy with steerable dish telescopes.

Below I am introducing to some commonly used concepts with respect to FRB astronomy, For detailed information reader can refer to “Fast Radio Bursts” by Petroff E. et al. 2019, 2021 and “Handbook of Pulsar Astronomy” by Lorimer and Kramer.

## 6.1 Propagation effects

### 6.1.1 Dispersion

When the light travels in the Intervening Medium due to electrons in the intervening medium the signal is delayed. This effect is frequency dependent. For a frequency of 1.4 GHz it is approximately (Petroff E. et al. 2019)

$$1.06 \left( \frac{\text{DM}}{500 \text{cm}^{-3} \text{pc}} \right) \left( \frac{\nu}{1.4, \text{GHz}} \right)^{-2} \text{sec} \quad (1)$$

Dispersion Measure or DM is a numerical measure of this delay. More the delay, more is the DM. Also it is related with distance of the source. For FRBs the DM components are due to Interstellar Medium, Inter Galactic Medium, Earth ionosphere etc. The Dispersive delay indicates that FRBs are extra galactic in nature.

### 6.1.2 Scintillation

Since, FRBs have small in size and the distance is extra galactic they forms very good point sources. Hence, Scintillation effects can be observed due to refractive and diffractive effects as the light passes through intervening medium.

### 6.1.3 Scattering

FRBs are usually very short interval phenomenon. They occur at millisecond duration. But they can be temporally broadened due to scattering. This leads to later TOA (Time of Arrival) for part of the signal that travelled longer path.

## 6.2 FRB models

Due to being a new subject and a transient phenomenon, for a long time there were just not enough candidates to justify any model of FRB. Hence, there exist many FRB models and not many have been rejected. Until release of first observation set by CHIME there were mostly few detected FRBs. With CHIME observations the number has increased exponentially. The observations points to two categories of FRBs, one off events and repeaters. Till 2019, there were not enough repeaters to hold the claim but with recent data release by chime the repeater count has increased to 50 (Andersen, B. C. et al., 2023). Also, some of the repeaters are found with periodic repeatability.

### 6.2.1 Neutron star progenitors

These forms the most majority of the models. Neutron stars gives rise to highly energetic phenomenons, The very high magnetic field of Neutron stars can be accounted for FRB emissions. Also, A class of Neutron stars pulsars have a similar phenomenon called Giant pulse, which is also random and more energetic than normal pulse. Few models also account for Supra massive Neutron stars and Magnetars.

#### a. Isolated Neutron star models

A number of theories (mostly those before 2019) argued FRBs to be generated due to Isolated Neutron stars. There are also two groups in it, One which supports radio emissions due to magnetosphere and another which supports for core collapse of Supra massive Neutron stars. But with increasing number of repeaters the core collapse idea is getting challenged. Also, since amount of energy release in FRBs is few orders more than normal Neutron stars, radio emissions due to magnetosphere is also questioned.

### **b. Interacting Neutron star models**

A few models suggests that FRBs are generated due to interaction between neutron star and another object in it surrounding. A model also suggests FRBs might be arising due to asteroids near Neutron stars.

### **c. Colliding Neutron star models**

A few neutron star models suggest the origin of phenomenon due to collision between neutron star and another compact object such as another neutron star or white dwarf.

#### **6.2.2 Black hole and White dwarf progenitor models**

Some of the theories points towards Black holes being te central engine for generation of FRB. While, there is no observable emission predicted for it. Also, Black hole mergers are supposed to be electromagnetically weak phenomenon.

The FRB emission is not possible with only white dwarf due to its less energy. But some models suggest an accretion of material from a white dwarf onto a Neutron star can produce a FRB.

# 7. Search for FRBs in uGMRT and SRT Observations

With New observation runs by CHIME telescope the rate of FRB detection has increased exponentially. CHIME helped detect both one off event FRBs and Repeaters. But for further studies of the sources CHIME does not have fine resolution observation capabilities. With increase in number of repeaters follow up searches started in with observatories. Follow up observations with better resolution telescopes gives important information about the localization, distance and flux of the Source. Out of all the repeaters only three have been found to be periodic in nature. FRB121102 was the first one to be noticed.

FRB180916 is another periodic repeater. It originates from a spiral galaxy (SDSS J015800.28+654253.0). It has observed periodicity of  $16.35 \pm 0.15$  days (Pilia M. 2021). It shows better activity at low radio frequencies. Hence, SRT (Sardinian Radio Telescope), uGMRT (upgraded Giant Meterwave Radio Telescope) and GBT (Green Bank Telescope) are three good telescopes to observe it.

There exists many pipelines to analyse the FRB observations. We have used SPANDAK pipeline (Gajjar et al. 2022). SPANDAK makes use of various pulsar and FRB data analysis software to effectively search for FRBs. It can also be used in machine learning mode. We will discuss about SPANDAK and other FRB software repository work in the next section.

## 7.1 RFI analysis

The first and most important step before searching FRBs is to identify and remove RFI (Radio Frequency Interference). While searching for FRBs we encounter FRB at both DM 0 and at higher DMs. The RFI at DM 0 is taken care by RFIFIND program from PRESTO (Ransom et al. 2002). RFIFIND identifies the RFI channels and creates a mask file for it. This mask file when applied to the observation dataset blocks the RFI channels. Further,

this mask information can be used with rfifind\_stats.py and weights\_to\_ignorechans.py from PRESTO to give information about channels to be blocked. These channels will be blocked while searching for FRB candidates. SPANDAK also performs a RFI quality check with its program.

## 7.2 Setting search Parameters

The search operation for FRBs is performed by Heimdall (Jameson A. et al.). Heimdall is a GPU accelerated pipeline which performs match filtering technique to find possible FRB candidates. Heimdall offers various parameters to improve your search. Few of the are

1. **dm\_tol** : This stands for DM tolerance while searching the dataset. It takes value from 1 and above. Finer the dm\_tol more better will be the search but also more intense the computing operation.
2. **snr\_cut** : FRBs are very high SNR (Signal to Noise Ratio) signals and hence searching for lower SNR signal is not necessary. Hence by setting this value to a required value we can speed up the process of search.
3. **boxcar\_max** : FRBs are also very short interval signals hence maximum width of the possible candidate can be set using this parameter.
4. **dm min max** : This is the option which lets you search for certain DMs rather than searching for full range. This is helpful while searching for FRB signature of a known repeater FRB.
5. **zap\_chans** : This uses the channel with RFI information given by SPANDAK RFI analysis and block those channels while performing candidate search.

There are few more parameters of both SPANDAK and Heimdall which can be found in the respective documentations.

### **7.3 Dedisperion**

As discussed section the dispersive delay is dependent of frequency and hence the Time of arrival for signal from same source at different frequency is different. To overcome this problem De-dispersioin technique is used. The DM of a new FRB is not known hence it needs to be done with trial method. One needs to take care of the narrow pulses not being missed. For known DM one can disable narrow pulses search with Heimdall. There are two types of Dedisperion methods - Coherent dedisperion and Incoherernt dedisperion. One can refer to “Handbook of Pulsar Astronomy” by Lorimer and Kramer for more details.

### **7.4 Detection of the Candidates**

Once the parameters are set Heimdall performs candidate search in the range with match filtering technique with defined boxcar width. This analysis is also called as “Single pulse search”. Once the Single pulse search candidates are identified, they are grouped together. This is a crucial step in the detection of FRBs. This is the step where the false signals are rejected. An artificial signal will have same signature at various time stamps and DMs in the signal. Hence, such signals are discarded. This is done by “frb\_detector.bl.py” program of SPANDAK.

### **7.5 Machine learning techniques**

Even after so much filtering the number of false alarms in a search are very high. Hence, to reduce more candidates few groups are using Machine learning techniques. Few of these are groups from CHIME, ASTRON and SETI. SPANDAK in SETI breakthrough listen program makes use of such algorithms.

## 7.6 Plotting of the candidates

Finally after reducing the candidates the possible candidates are plotted on a waterfall plot such as in fig 21. SPANDAK has “waterfaller\_vg.py” program which has parameters to plot the signature of the pulse in both dedispersed and normal mode. It also applied statistical analysis to flag the possible candidate. Below is an example of a FRB signature detected by SRT (Sardinian Radio Telescope) of FRB180916.

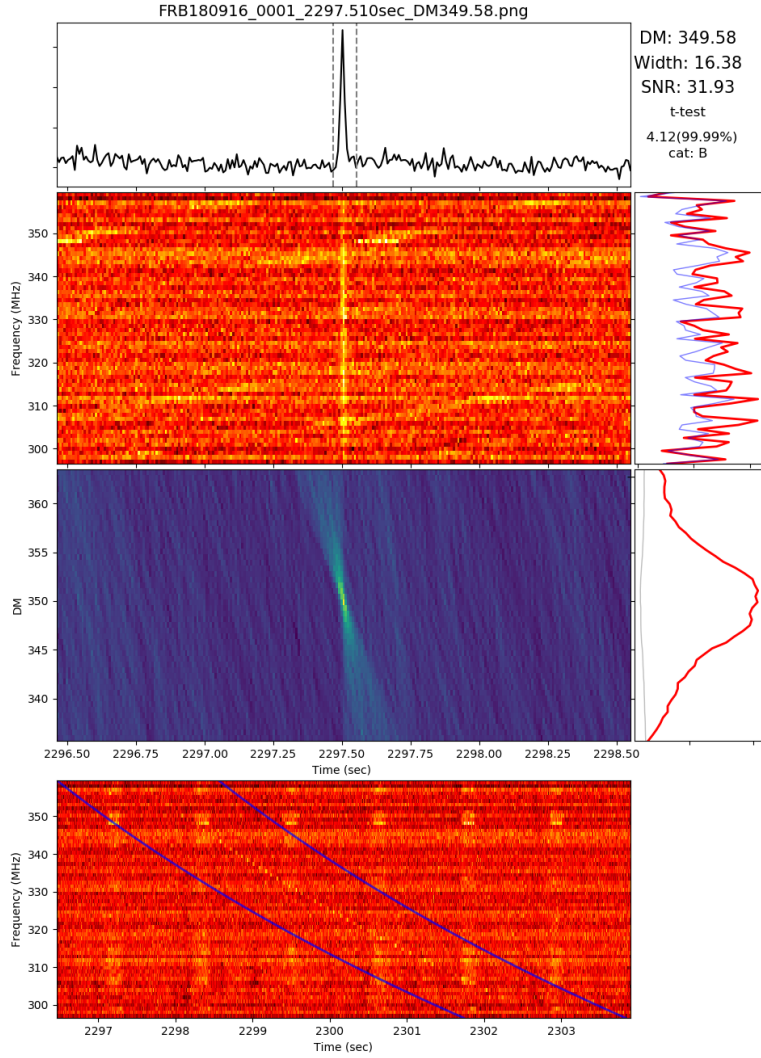


**Fig. 26.** FRB180916 observed by SRT

## 8. FRB Software Jungle

FRB is a comparatively new field. Also, it has originated from Pulsar surveys. Hence, most of the FRB pipelines are based on Pulsar pipelines. Pulsar pipelines have more sophisticated and proven algorithms which are continued to be used in FRBs. FRB pipelines are built on top of pulsar pipelines and hence this creates a problem of installing all the required pulsar pipelines to work on FRB data. I've used below three pipelines for the search of FRBs.

1. **PRESTO** : PRESTO (Ransom et al. 2002) is a very good pipeline for searching FRBs. It has excellent RFI analysis, dedispersion, single pulse search tools. The problem with PRESTO was a single thread program for a long time. It is now can be used upto 4 CPU cores and hence it is very slow. Also, in search process it produces enormous amount of files. FRBs needs active monitoring and hence PRESTO is too slow for online search. It is still used for the offline search because it is still one of the best.
2. **Heimdall** : Heimdall (Jameson A. et. al) is a GPU accelerated pipeline for FRB searches. It uses parallel processing and is very fast compared to PRESTO. But Heimdall is not as accurate as PRESTO's `single_pulse_search.py` in FRB searches. Hence, it is mostly useful to detect strong FRBs and active monitoring due to very fast speed of processing. Heimdall is based on CUDA (NVIDIA) and hence needs user to have NVIDIA GPU system. Also, a good memory to do finer analysis.
3. **SPANDAK** : SPANDAK (Gajjar et al. 2022) is a pipeline which makes use of good properties of both PRESTO and Heimdall to get an optimal result. Its Machine learning algorithms are really speed up the search of FRB. SPANDAK can be used in both CPU and GPU mode. But it also has its limitations. SPANDAK is based on Python 2.7 and needs many pulsar repositories to be installed. With Python 2 discontin-

ued and related packages also upgrading to Python 3. It is getting difficult to install SPANDAK on a modern Linux system.

Below is the list of software (apart from apt libraries and packages) which needs to be compiled from source and installed before working,

1. FFTW3
2. CFITSIO (NASA)
3. PSRCAT (ATNF)
4. TEMPO (NANOGRAV)
5. PRESTO (Python 2 version)
6. TEMPO2
7. PSRCHIVE
8. DSPSR
9. CUDA (NVIDIA)
10. Dedisp
11. PSRDADA
12. Heimdall
13. Sigproc (Mike Keith)
14. Sigpyproc (Ewin Barr)
15. Gnuplot-py (Michael Haggerty)

# **9. By Products of FRB Analysis**

## **9.1 Manual for installing SPANDAK on a latest Linux system**

In order to reduce efforts in installing SPANDAK for other users. I compiled a manual with step by step instruction to install SPANDAK on a Linux system. It has been updated and put on the github repository of SPANDAK with credits to me by Dr. Vishal Gajjar.

## **9.2 Common installer for Pulsar and and FRB repositories**

Installation of source software has been a very tedious work in Pulsar Astronomy and it lacks a common installer such as HEASOFT. PSRSOFT by Mike Keith was an excellent option for it but it also needs to be updated. I have started working on this common installer and it will soon be available.

## **9.3 SPANDAK3**

Python 2 has been outdated by latest Linux systems and Python2 packages and even Pip2 is not available on easy to install package managers like ‘apt’. Hence, there is a need to update SPANDAK from Python2 to Python3. I have developed base of all dependencies of SPANDAK on Python 3 and has translated few programs like frb\_detector.bl.py (with full success) and SPANDAK (with partial success).

# Acknowledgements

I would like to thank Prof. T.R. Seshadri and Prof. H.P. Singh for giving me opportunity to work on this topic. Special thanks to the full team of Radio lab Prof. Chetana Jain, Prof. Suprit Singh, Priya, Rajat and Sachin. Thank you to IUCAA RPL team Prof. Dhruba Saikia, Prof. Avinash Deshpande, Ashish Mhaske and Jameer Manur for the guidance while working on Horn antenna.

I would like to thank Dr. Maura Pilia (INAF, Italy) for guidance though out the Second part. Thank you to Dr. Alessandro Rifolfi and INAF team for providing access to computer cluster at Cagliari for the analysis. I am thankful to Prof. T.R. Seshadri and Prof. Patrick Das Gupta for fruitful discussions on FRBs. I am also thankful to my friend Pankaj for discussions on FRBs and Anmol for providing access to his computer for running analysis locally. I would also like to thank Dr. Vishal Gajjar for help during installation of SPANDAK.

# References

1. Lorimer et al., 2007 A Bright Millisecond Radio Burst of Extragalactic Origin
2. Andersen, B. C. et al., 2023 CHIME/FRB Discovery of 25 Repeating Fast Radio Burst Sources
3. Mhaske A. et al., 2022 A Bose Horn Antenna Radio Telescope (BHARAT) design for 21 cm hydrogen line experiments for radio astronomy teaching
4. [Low Frequency Radio Astronomy a.k.a. blue-book - NCRA-TIFR](#)
5. Patel N. A., Patel R. N. et al., A low-cost 21 cm horn-antenna radio telescope for education and outreach
6. Ruta Kale et al., October 2020 CAPTURE: a continuum imaging pipeline for the uGMRT
7. Ransom et al. 2002 PRESTO
8. Petroff E. et al. 2019 Fast Radio Bursts
9. Petroff E. et al. 2021 Fast Radio Bursts at the dawn of the 2020s
10. Gajjar et al. 2022 Searching for Broadband Pulsed Beacons from 1883 Stars Using Neural Networks